Advances in Nano Research, *Vol. 11, No. 6 (2021) 641-648*
https://doi.org/10.12989/anr.2021.11.6.641

The determination of effect of TiO_2 on dynamic behavior of scaled concrete structure by OMA

Sertaç Tuhta*

Ondokuz Mayis University, Faculty of Engineering, Department of Civil Engineering, Atakum/Samsun, Turkey

(*Received February 7, 2020, Revised October 2, 2021, Accepted October 6, 2021*)

Abstract. In this article, the dynamic parameters (frequencies, mode shapes, damping ratios) of the scaled concrete structure and the dynamic parameters (frequencies, mode shapes, damping ratios) of the entire outer surface of titanium dioxide, 80 micron in thickness are compared using operational modal analysis method. Ambient excitation was provided from micro tremor ambient vibration data on ground level. Enhanced Frequency Domain Decomposition (EFDD) was used for the output only modal identification. From this study, a good correlation between mode shapes was found. Titanium dioxide applied to the entire outer surface of the scaled concrete structure has an average of 11.78% difference in frequency values and 10.15% in damping ratios, proving that nanomaterials can be used to increase rigidity in structures, in other words, for reinforcement. Another important result determined in the study was the observation of the adherence of titanium dioxide and similar nanomaterials mentioned in the introduction to concrete structure surfaces was at the highest level.
Keywords: EFDD; modal parameter; nanomaterial; operational modal analysis; TiO_2

1. Introduction

Since nanotechnology is an ever-evolving field, it is difficult to make a general definition. However, according to the definition that everyone agrees on, the production of materials and devices by controlling the substance is called nanotechnology. At the level of atoms, molecules and supramolecular (nanoscale) structures, in other words, it is possible to express it as the use of very small material particles to produce new large-scale materials. The products obtained using nanotechnologies are called nanomaterials. Depending on the size, nanotechnology is defined as the study and use of structures between 1 nanometer (nm) and 100 nanometers in size. Various issues take place in nano-level processing, such as gravity becomes insignificant, electrostatic forces and quantum effects come into being. Another important point is that as a result of the use of particles in the nanoscale, the ratio of the atoms on the surface increases compared to the ones inside, causing the material properties to change. Nanotechnology can produce materials with many unique properties that can improve existing building materials: lighter and stronger structural composites, less maintenance coatings, more useful cement-based materials, products with better thermal insulation properties, etc. can be listed. The use of nanomaterials in the composition of some materials such as cement, concrete, etc. will be beneficial in air conditioning and energy efficiency. In addition, nanomaterials applied to the surfaces of structural elements of buildings can contribute to environmental cleaning and energy generation through photocatalytic reactions Akbaş (2020). Thanks to nanotechnology, concrete can be stronger, more durable and easier to place, steel can be made tougher, self-cleaning glass, and paints can be made more insulating and water-repellent. Nanomaterials and nanotechnologies have attracted considerable scientific interest due to new potential uses of nanometer-scale particles and hence the large amount of funding and effort. Compared to other large industrial sectors, the construction industry has lagged behind in its potential to benefit from nanotechnology. Reports on the use of nanotechnology in construction materials, potential uses of nanotechnology in terms of the construction and development of building materials are listed as follows: Using nanoparticles, carbon nanotubes and nanofibers to increase the strength and durability of cement composites and to reduce environmental pollution, cheap and corrosion-free steel production, product production with ten times the performance of existing thermal insulation materials, the production of coatings that enables self-cleaning and self-color change to minimize energy consumption. The use of nanotechnological materials in buildings not only helps to increase their life span, but also enables them to react to different factors such as the reduction of energy they spend, fire resistance and corrosion. Nano-silica shortens the setting time of mortar compared to silica fume (microsilica) and reduces mixing water and segregation by improving cohesion (Zhang *et al*. 2020, 2021), (Wang *et al*. 2021a, b). Current researchers interested in nanoscience and nanotechnologies are extensively investigating these new properties (Eltaher *et al*. 2019). Because macro properties can change at the nanoscale it is possible to produce significantly new materials and processes. Discussions on the application of nanotechnology in civil engineering, especially in construction, are extremely important. However, many of the advances in nanotechnology have the potential to be

*Corresponding author, Assistant Professor,
E-mail: stuhta@omu.edu.tr

ISSN: 2287-237X (Print), 2287-2388 (Online)

applied in the civil engineering field. The use of nanotechnological materials in buildings not only helps to increase their life span, but also enables them to react to different factors such as the consumption of energy they spend, fire resistance and corrosion. Various negativities that occur with time in building elements can be avoided by using nanotechnological materials (self-healing and waterproof concrete, self-cleaning plaster, etc.) Eren and Aydogdu (2018). In the light of the information mentioned above, carbon nanotubes, one of the most used nanomaterials in the field of civil engineering, are in the form of a cylindrical carbon and it takes its name from the nanometer diameter. They can be several millimeters in lenght and have a "layer" or wall (single wall nanotube) or multiple walls (multi-wall nanotubes) (Uzun and Civalek 2019, Civalek *et al*. 2020). Nanotubes have superior strength and unique electrical properties, as well as efficient thermal properties. It is very popular due to its properties. Another nanomaterial, titanium dioxide nanoparticles, is added to concrete to improve its properties. This white pigment is used as a very good reflective coating or added to paints, cement and windows for its sterilizing properties. Titanium dioxide breaks down organic pollutants, volatile organic compounds and bacterial membranes through powerful photocatalytic reactions and reduces the proportion of air pollutants when applied to external surfaces. As it is hydrophilic, it provides self-cleaning feature to the applied surfaces. The concrete surfaces obtained have a white color that preserves their whiteness very effectively. Silicon dioxide particles, on the other hand, have the ability to increase the compressive strength significantly. By filling the pores between large fly ash and cement particles, they allow the production of concrete containing large fly ash volumes at an early age. Nano-silica shortens the setting time of mortar compared to silica fume (microsilica) and reduces mixing water and segregation by improving cohesion (Ma *et al*. 2016, Wang *et al*. 2020a, b). Zinc oxides are preferred because of their semiconductor and piezoelectric properties. In building materials, they are added to a variety of products, including plastics, ceramics, glass, cement, rubber, paints, adhesives, sealants, pigments, flame retardants. Zinc oxide used in concrete production improves concrete's processing time and its resistance to water. Another nanomaterial, alumina, reacts with calcium hydroxide produced from hydration of calcium silicates. The rate of pozzolanic reaction is proportional to the amount of surface area available for the reaction. The addition of high purity nano-alumina improves the properties of concretes in terms of higher tensile stress and flexural strength. Cement can advantageously be displaced in the concrete mix with nano-alumina particles up to a maximum limit of 2.0% with average particle sizes of 15 nm; optimum nano-alumina particle content is achieved with 1.0% replacement. When the academic studies conducted so far are examined, it has been determined that there is no significant accumulation of nanomaterials in the field of applied civil engineering (Pandey *et al*. 2019). For this reason, a study that has no examples in the literature was conducted on this study. The dynamic parameters (frequencies, mode shapes, damping ratios) of a scaled concrete structure were found by the operational modal analysis method. In the continuation of the research, the upper surface of this structure was coated with titanium dioxide (80 micron), and its dynamic parameters (frequencies, mode shapes, damping ratios) were found again by operational modal analysis method and compared. The reason for using titanium dioxide in the study is that its mechanical properties are as good as conventional materials (AFRP, BFRP, CFRP, GFRP, etc.) used in reinforcement. Thanks to the research, details that will help people who work on this subject are included. The use of other nanomaterials such as titanium dioxide as a reinforcement element in concrete, reinforced concrete, steel, composite-type structures is being investigated, and the results of these studies will be presented later.

Ambient vibration testing (also called Operational Modal Analysis) is the most economical, non-destructive testing method to acquire vibration data from large civil engineering structures for Output-Only Modal Identification. General characteristics of structural response (appropriate frequency, displacement, velocity, acceleration), suggested measuring quantity (such as velocity or acceleration) depends on the type of vibrations (Traffic, Acoustic, Machinery inside, Earthquakes, Wind…) are given in Vibration of Buildings (1990).

In general, operational modal analysis is used to determine the damage levels of the existing structures, to check the validity of the assumptions made while constructing the finite element model, to update the initial numerical model of the existing structures according to the experimental data, to determine the dynamic characteristics of the structures by the experimental modal analysis method when the numerical model of the existing structures cannot be formed and to follow the structural health is widely used in the process (Alvin and Park 1994, Tseng *et al*. 1994, Aliev and Larin 1998, Ljung 1999, Lus *et al*. 2003, Roeck (2003). It was observed that three types of definitions were used in the engineering structures: modal parameter identification; structural-modal parameter identification; control-model identification methods. In the frequency domain, the system identification is based on the singular value decomposition of the spectral density matrix and it is denoted as Frequency Domain Decomposition (FDD) and its further development is called Enhanced Frequency Domain Decomposition (EFDD). In the time domain there are three different implementations of the Stochastic Subspace Identification (SSI) technique: Unweighted Principal Component (UPC); Principal component (PC); Canonical Variety Analysis (CVA) is used for the modal updating of the structure (Sestieri and Ibrahim 1994, Balmes 1997, Bendat 1998, Marwala 2010).

It is necessary to estimate the sensitivity of the reaction of the examined system to change the random or fuzzy parameters of a structure. Investigated measurement noise perturbation influences to the identified system modal and physical parameters. Estimated measurement noise border, for which identified system parameters are acceptable for validation of finite element model of examine system. System identification is realized by observer Kalman filter Kalman (1960), Trifunac (1972), Ibrahim (1977) and Juang

(1994) Subspace, algorithms. In special case observer gain may be coincide with the Kalman gain. Stochastic state-space model of the structure are simulated by Monte-Carlo method. As a result of these theoretical and experimental studies, the importance of temperature change and humidity has emerged once again from the environmental factors affecting the modal parameters. The effects of temperature and humidity on modal parameters have been the subject of thorough examination in the last 15 years Kasımzade and Tuhta (2017, 2018, 2019).

For this purpose, the dynamic parameters (frequencies, mode shapes, damping ratios) of the scaled concrete structure and the dynamic parameters (frequencies, mode shapes, damping ratios) of the entire outer surface of the 80 micron thick titanium dioxide are compared using the operational modal analysis method. Ambient excitation was provided from the recorded micro tremor ambient vibration data on ground level. Enhanced Frequency Domain Decomposition (EFDD) is used for the output only modal identification.

2. Modal parameter extractions (EFDD)

The (FDD) ambient modal identification is an extension of the Basic Frequency Domain (BFD) technique or called the Peak-Picking technique. This method uses the fact that modes can be estimated from the spectral densities calculated, in the case of a white noise input, and a lightly damped structure. It is a non parametric technique that determines the modal parameters directly from signal processing. The FDD technique estimates the modes using a Singular Value Decomposition (SVD) of each of the measurement data sets. This decomposition corresponds to a Single Degree of Freedom (SDOF) identification of the measured system for each singular value (Brincker *et al*. 2000). The Enhanced Frequency Domain Decomposition technique is an extension to Frequency Domain Decomposition (FDD) technique. This technique is a simple technique that is extremely basic to use. In this technique, modes are easily picked locating the peaks in Singular Value Decomposition (SVD) plots calculated from the spectral density spectra of the responses. FDD technique is based on using a single frequency line from the Fast Fourier Transform analysis (FFT), the accuracy of the estimated natural frequency based on the FFT resolution and no modal damping is calculated. On the other hand, EFDD technique gives an advanced estimation of both the natural frequencies, the mode shapes and includes the damping ratios (Jacobsen *et al*. 2006). In EFDD technique, the single degree of freedom (SDOF) Power Spectral Density (PSD) function, identified about a peak of resonance, is taken back to the time domain using the Inverse Discrete Fourier Transform (IDFT). The natural frequency is acquired by defining the number of zero crossing as a function of time, and the damping by the logarithmic decrement of the correspondent single degree of freedom (SDOF) normalized auto correlation function Peeters (2000). In this study modal parameter identification was implemented by the Enhanced Frequency Domain Decomposition. The relationship between the input and responses in the EFDD technique can be written as, in this method, unknown input is represented with $x(t)$ and measured output is represented with $y(t)$

$$\left[G_{yy}(j\omega)\right]=[H(j\omega)]^{*}[G_{xx}(j\omega)][H(j\omega)]^{T} \tag{1}$$

where $G_{xx}(j\omega)$ is the $r\,x\,r$ Power Spectral Density (PSD) matrix of the input. $G_{yy}(j\omega)$ is the $m\,x\,m$ Power Spectral Density (PSD) matrix of the output, $H(j\omega)$ is the $m\,x\,r$ Frequency Response Function (FRF) matrix, and * and superscript T denote complex conjugate and transpose, respectively. The FRF can be reduced to a pole/residue form as follows:

$$[H(\omega)]=\frac{[Y(\omega)]}{[X(\omega)]}=\sum_{k=1}^{m}\frac{[R_k]}{j\omega-\lambda_k}+\frac{[R_k]^{*}}{j\omega-\lambda_k^{*}} \tag{2}$$

where n is the number of modes λ_k is the pole and, R_k is the residue. Then Eq. (1) becomes as:

$$G_{yy}(j\omega)=\sum_{k=1}^{n}\sum_{s=1}^{n}\left[\frac{[R_k]}{j\omega-\lambda_k}+\frac{[R_k]^{*}}{j\omega-\lambda_k^{*}}\right] G_{xx}(j\omega)\left[\frac{[R_s]}{j\omega-\lambda_s}+\frac{[R_s]^{*}}{j\omega-\lambda_s^{*}}\right]^{\bar{H}} \tag{3}$$

where s the singular values, superscript is H denotes complex conjugate and transpose. Multiplying the two partial fraction factors and making use of the Heaviside partial fraction theorem, after some mathematical manipulations, the output PSD can be reduced to a pole/residue form as fallows;

$$\left[G_{yy}(j\omega)\right]=\sum_{k=1}^{n}\frac{[A_k]}{j\omega-\lambda_k}+\frac{[A_k]^{*}}{j\omega-\lambda_k^{*}}+\frac{[B_k]}{-j\omega-\lambda_k}+\frac{[B_k]^{*}}{-j\omega-\lambda_k^{*}} \tag{4}$$

where A_k is the k th residue matrix of the output PSD. In the EFDD identification, the first step is to estimate the PSD matrix. The estimation of the output PSD known at discrete frequencies is then decomposed by taking the SVD (singular value decomposition) of the matrix;

$$G_{yy}(j\omega_i)=U_iS_iU_i^{\bar{H}} \tag{5}$$

where the matrix $U_i=[u_{i1},u_{i2},\ldots,u_{im}]$ is a unitary matrix holding the singular vectors u_{ij} and s_{ij} is a diagonal matrix holding the scalar singular values. The first singular vector u_{ij} is an estimation of the mode shape. PSD function is identified around the peak by comparing the mode shape estimation u_{ij} with the singular vectors for the frequency lines around the peak. From the piece of the SDOF density function obtained around the peak of the PSD, the natural frequency and the damping can be obtained.

3. Description of the scaled concrete structure

The scaled concrete structure was obtained in the Ondokuz Mayıs University Civil Engineering Laboratory. The mechanical properties of the concrete used are as follows: modulus of elasticity E = 2.80E10 N/m^2, Poisson ratio μ = 0.2, mass per unit volume ρ = 24000 N/m^3. The dimensions of the building are shown in Fig. 1.

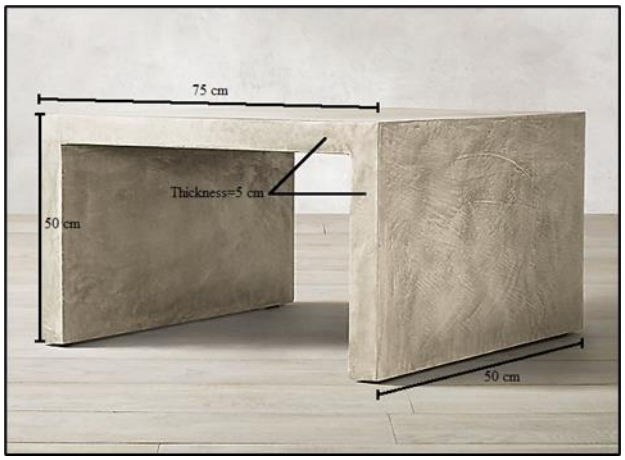

Fig. 1 Illustration of the scaled concrete structure

(a) First setup

(b) Second setup

Fig. 2 The accelerometers location of the experimental model in the 3D view

4. Operational modal analysis of the scaled concrete structure

Three accelerometers were used to measure ambient vibrations. One of them is always assigned as the reference sensor located at the bottom of shear wall. The acceleration record was measured in two data sets. For the two data sets, 2 and 3 accelerometers were used, respectively.

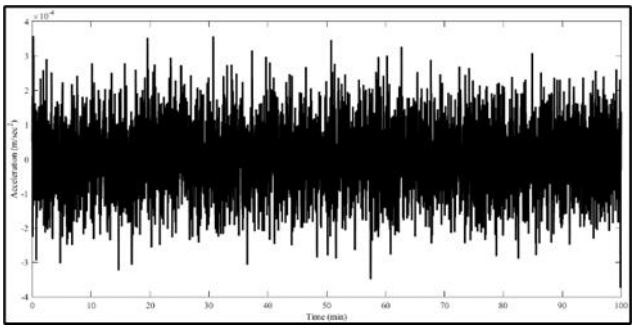

Fig. 3 Ambient excitation data from the recorded micro tremor data on ground level x axis-time (min), y axis-acceleration (m/sec^2)

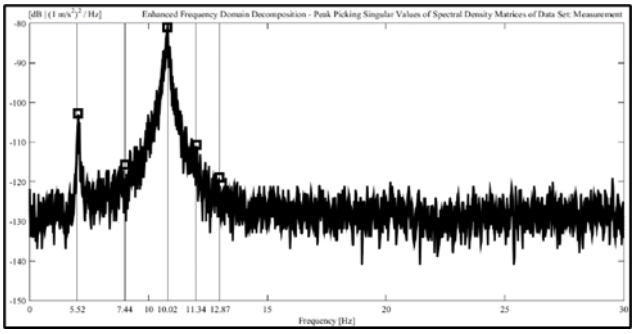

Fig. 4 Singular values of spectral density matrices (scaled concrete structure) x axis-frequency (hz), y axis-[db|(1 m/s^2)^2/hz]

Accelerometers were calibrated and used, thus preventing possible measurement errors. 100 minutes were recorded for each data set. Selected measurement points and directions are shown in the figure. Ambient simulation was achieved using microtremor data recorded at ground level.

After the first data set measurement, the accelerometers were recalibrated. The acceleration records of the first data set were saved in the folder for analysis. Before starting the second data set measurement, all connections were rechecked.

The data acquisition computer provides the ambient vibration records. During measurements, the data files from the previous setup are transferred to the computer for data analysis by using a software package. However, in case there is a display of unexpected signal drifts or unwanted noise or corrupted for some unknown reasons, the data set must be discarded and measurements be repeated.

Before measurements were made, the cable used to connect the sensors to the data acquisition equipment must be laid out. Following each measurement, the roving sensors are systematically located from floor to floor until the test is completed (Figs. 2(a) and 2(b)). The equipment used for the measurement includes three Sensebox accelerometers (with both x and y directional measurements) and Güralp systems seismometer and Matlab Data acquisition toolbox. For modal parameter estimation from the ambient vibration data, the operational modal analysis (OMA) software ARTeMIS Extractor (1999) is used. The Eigen frequencies were found as the peaks of non-parametric spectrum estimates when the simple peak-picking method (PPM) was used. This frequency selection

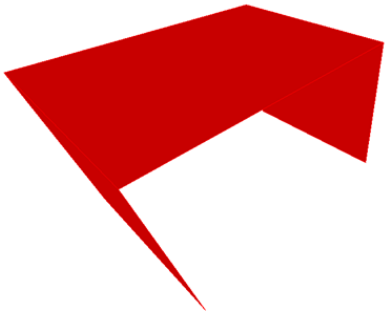

1st Mode shape (f = 5.52 Hz, ξ = 1.02)

2nd Mode shape (f = 7.44 Hz, ξ = 0.86)

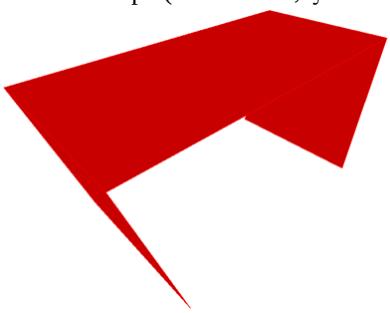

3rd Mode shape (f = 10.02 Hz, ξ = 0.69)

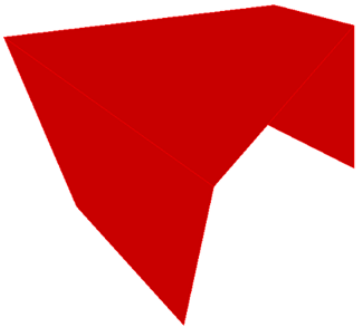

4th Mode shape (f = 11.34 Hz, ξ = 0.80)

5th Mode shape (f = 12.87 Hz, ξ = 0.62)

Fig. 5 Experimentally identified mode shapes of the scaled concrete structure

Table 1 Operational modal analysis result at the scaled concrete structure

Mode number	1	2	3	4	5
Frequency (Hz)	5.52	7.44	10.02	11.34	12.87
Modal damping ratio (ξ)	1.02	0.86	0.69	0.80	0.62

Fig. 6 Materials and equipment used in coating application

procedure became a subjective task in case of noisy test data, weakly excited modes and relatively close Eigen frequencies. Also for damping ratio estimation, the related half-power bandwidth method was not favorable. This why the most popular and useful algorithm to use is Frequency Domain Decomposition (FDD), because of its convenience and operating speed.

Singular values of spectral density matrices, attained from vibration data using PP (Peak Picking) technique were shown in Fig. 4. Natural frequencies acquired from all measurement setup were given in Table 1. The first five mode shapes extracted from experimental modal analyses were given in Fig. 5. When all measurements were examined, it could be seen that a good accordance was found between experimental mode shapes. In addition, when both setup sets were experimentally identified modal parameters were checked with each other, it could be seen that there was a best agreement between the mode shapes in the experimental modal analyses.

5. Operational modal analysis of the coated scaled concrete structure

In the case of the coated scaled concrete structure, the following studies were made on it to check and examine the efficiency of using TiO_2 coating: the entire outer surface of the 80 micron thick of the structure were coated with multi-layer TiO_2 coating. TiO_2 coating and its components YKS is a product of YKS (Yapı Kimyasalları Sanayi) corporation, Bosch branded PFS2000 model spray equipment was used in the coating application (Fig. 6). The properties of the TiO_2 coating are: E = 23E10 N/m^2, Poisson ratio μ = 0.27, mass per unit volume ρ = 40000 N/m^3, thickness = 0.00008 m.

The entire outer surface of the scaled concrete structure is covered with many layers of titanium dioxide. The surface is expected to dry during each application. approximately 1hour of curing in order to prepare a surface

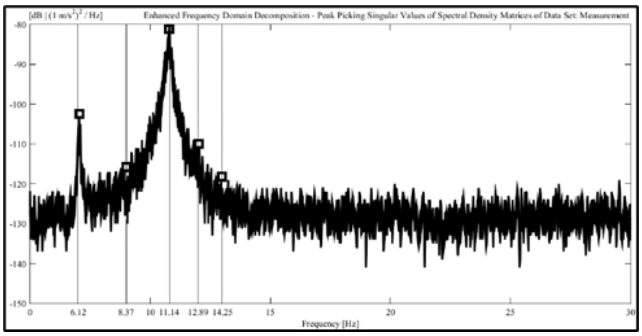

Fig. 7 Singular values of spectral density matrices (coated scaled concrete structure) x axis-frequency (hz), y axis-[db|(1 m/s^2)^2/hz]

Table 2 Operational modal analysis result at the coated scaled concrete structure

Mode number	1	2	3	4	5
Frequency (Hz)	5.52	7.44	10.02	11.34	12.87
Modal damping ratio (ξ)	1.02	0.86	0.69	0.80	0.62

Table 3 Comparison of the existing and the coated structures frequency results

Mode number	1	2	3	4	5
Frequency (Hz)-E	5.52	7.44	10.02	11.34	12.87
Frequency (Hz)-C	6.12	8.37	11.14	12.89	14.25
Difference (%)	10.86	12.50	11.17	13.66	10.72

Table 4 Comparison of the existing and the coated structures damping ratio results

Mode number	1	2	3	4	5
Modal damping ratio (ξ)-E	1.02	0.86	0.69	0.80	0.62
Modal damping ratio (ξ)-C	0.95	0.83	0.60	0.71	0.52
Difference (%)	6.86	3.48	13.04	11.25	16.12

for application of titanium dioxide. After these setups, ambient vibration tests are followed by curing to obtain experimental dynamic characteristics similar to previously used properties in order to obtain comparative measurements. SVSDM are shown in Fig. 7. Table 2 shows the identified natural frequencies and modal damping ratios.

It is clear that using titanium dioxide seems to be very effective for strengthening concrete members along with increasing stiffness; this research aims to determine how TiO_2 implementation affects structural response of the scaled concrete structure by changing its dynamic characteristics.

6. Conclusions

In this study, operational modal analysis of the existing and titanium dioxide coated scaled concrete structure was performed and the results were evaluated. In the comparison of the result of this study, the followings were observed:

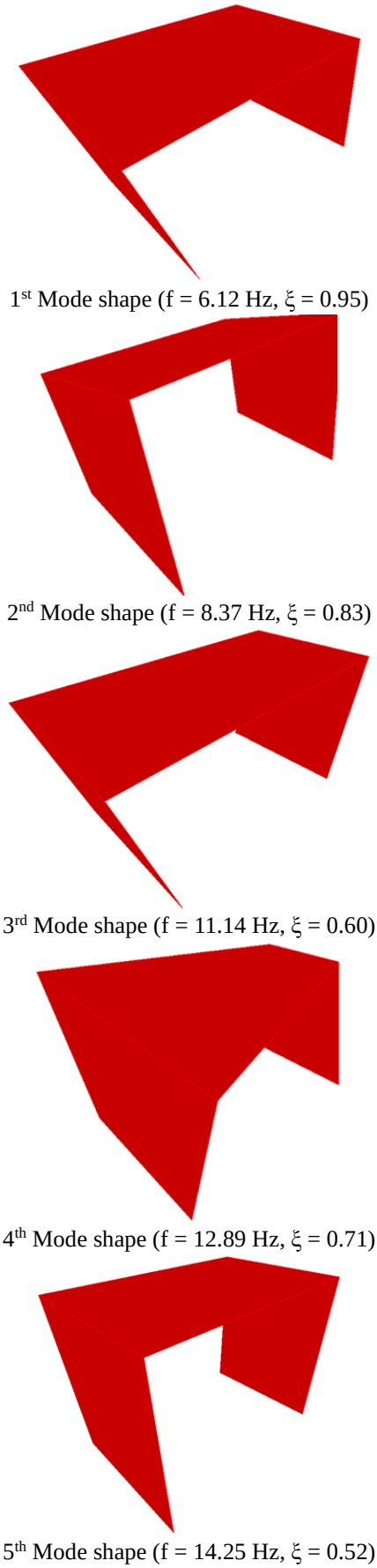

1st Mode shape (f = 6.12 Hz, ξ = 0.95)

2nd Mode shape (f = 8.37 Hz, ξ = 0.83)

3rd Mode shape (f = 11.14 Hz, ξ = 0.60)

4th Mode shape (f = 12.89 Hz, ξ = 0.71)

5th Mode shape (f = 14.25 Hz, ξ = 0.52)

Fig. 8 Experimentally identified mode shapes of the coated scaled concrete structure

• From the ambient vibration test, the first five natural frequencies are attained experimentally, which range between 5 and 15 Hz.

• When comparing the existing and the coated scaled concrete structure results, it is clearly seen that there is a good agreement between mode shapes.

• It has been determined that there is an average of 11.78% difference between the frequency values of the existing scaled concrete structure and the titanium dioxide coated scale concrete structure.

• It has been determined that there is an average of 10.15% difference between the damping ratios of the existing scale concrete structure and the titanium dioxide coated scale concrete structure.

• Titanium dioxide applied to the entire outer surface (80 micron thick) of the scaled concrete structure has an average of 11.78% difference in frequency values (Table 3) and 10.15% in damping ratios (Table 4), proving that nanomaterials can be used to increase rigidity in structures, in other words, for reinforcement.

• Another important result determined in the study is the observation of the adherence of titanium dioxide and similar nanomaterials mentioned in the introduction to concrete structure surfaces was at the highest level.

References

Akbaş, Ş.D. (2020), "Modal analysis of viscoelastic nanorods under an axially harmonic load", *Adv. Nano Res.*, **8**(4), 277-282. https://doi.org/10.12989/anr.2020.8.4.277.

Aliev, F.A. and Larin, V.B. (1998), *Optimization of Linear Control Systems: Analytical Methods and Computational Algorithms*, CRC Press.

Alvin, K.F. and Park, K.C. (1994), "Second-order structural identification procedure via state-space-based system identification", *AIAA J.*, **32**(2), 397-406. https://doi.org/10.2514/3.11997.

ANSI S2.47 (1990), Vibration of buildings-guidelines for the measurement of vibrations and evaluation of their effects on buildings, American National Standards Institute; Washington, DC, U.S.A.

ARTeMIS Extractor, (1999), *Structural Vibration Solutions*, Aalborg, Denmark.

Balmes, E. (1997), "New results on the identification of normal modes from experimental complex modes", *Mech. Syst. Signal Pr.*, **11**(2), 229-243. https://doi.org/10.1006/mssp.1996.0058.

Bendat, J.S. (1998), *Nonlinear Systems Techniques and Applications*, Wiley.

Brincker, R., Zhang, L. and Andersen, P. (2000), "Modal identification from ambient responses using frequency domain decomposition", *Proceedings of the 18th International Modal Analysis Conference* (*IMAC)*, San Antonio, Texas, USA, February.

Civalek, O., Uzun, B. and Yayli, M.O. (2020), "Frequency, bending and buckling loads of nanobeams with different cross sections", *Adv. Nano Res.*, **9**(2), 91-104. https://doi.org/10.12989/anr.2020.9.2.091.

Eltaher, M.A., Almalki, T.A., Ahmed, K.I. and Almitani, K.H. (2019), "Characterization and behaviors of single walled carbon nanotube y quivalent-continuum mechanics approach", *Adv. Nano Res.*, **7**(1), 39-49. https://doi.org/10.12989/anr.2020.9.1.059.

Eren, M. and Aydogdu, M. (2018), "Finite strain nonlinear longitudinal vibration of nanorods", *Adv. Nano Res.*, **6**(4), 323-337. https://doi.org/10.12989/anr.2018.6.4.323.

Ibrahim, S.R. (1977), "Random decrement technique for modal identification of structures", *J. Spacecraft. Rockets*, **14**(11), 696-700. https://doi.org/10.2514/3.57251.

Jacobsen, N.J., Andersen, P., and Brincker, R. (2006), "Using enhanced frequency domain decomposition as a robust technique to harmonic excitation in operational modal analysis", *Proceeding of International Conference on Noise and Vibration Engineering* (*ISMA)*, Leuven, Belgium, September.

Juang, J.N. (1994), *Applied System Identification*, Prentice Hall.

Kalman, R.E. (1960), "A new approach to linear filtering and prediction problems", *J. Basic Eng.*, **82**(1), 35-45. https://doi.org/10.1115/1.3662552.

Kasimzade, A.A. and Tuhta, S. (2017), "Application of OMA on the bench-scale earthquake simulator using micro tremor data", *Struct. Eng. Mech.*, **61**(2), 267-274. https://doi.org/10.12989/sem.2017.61.2.267.

Kasimzade, A.A. and Tuhta, S. (2017), "OMA of model steel structure retrofitted with CFRP using earthquake simulator", *Earthq. Struct.*, **12**(6), 689-697. https://doi.org/10.12989/eas.2017.12.6.689.

Ljung, L. (1999), *System Identification: Theory for the User*, Prentice Hall.

Lus, H., De Angelis, M., Betti, R. and Longman, R.W. (2003), "Constructing second-order models of mechanical systems from identified state space realizations. Part I: Theoretical discussions", *J. Eng. Mech.*, **129**(5), 477-488. https://doi.org/10.1061/(ASCE)0733-9399(2003)129:5(477).

Ma, B., Li, H., Li, X., Mei, J. and Lv, Y. (2016), "Influence of nano-TiO_2 on physical and hydration characteristics of fly ash–cement systems", *Constr. Build. Mater.*, **122**, 242-253. https://doi.org/10.1016/j.conbuildmat.2016.02.087.

Marwala, T. (2010), *Finite Element Model Updating Using Computational Intelligence Techniques: Applications to Structural Dynamics*, Springer Science-Business Media.

Pandey, H.K., Hirwani, C.K., Sharma, N., Katariya, P.V., Dewangan, H.C. and Panda, S.K. (2019), "Effect of nano glass cenosphere filler on hybrid composite eigenfrequency responses-An FEM approach and experimental verification", *Adv. Nano Res.*, **7**(6), 419-429. https://doi.org/10.12989/anr.2019.7.6.419.

Peeters, B. (2000), "System identification and damage detection in civil engineering", Ph.D. Dissertation, Katholieke Universiteit Leuven, Leuven, Belgium.

Roeck, G.D. (2003), "The state-of-the-art of damage detection by vibration monitoring: the SIMCES experience", *J. Struct. Control*, **10**(2), 127-134. https://doi.org/10.1002/stc.20.

Sestieri, A. and Ibrahim, S.R. (1994), "Analysis of errors and approximations in the use of modal coordinates", *J. Sound Vib.*, **177**(2), 145-157. https://doi.org/10.1006/jsvi.1994.1424.

Trifunac, M.D. (1972), "Comparisons between ambient and forced vibration experiments", *Earthq. Eng. Struct. D.*, **1**(2), 133-150. https://doi.org/10.1002/eqe.4290010203.

Tseng, D.H., Longman, R.W. and Juang, J.N. (1994), "Identification of the structure of the damping matrix in second order mechanical systems", *Spaceflight Mech.*, 167-190.

Tuhta, S. (2018), "GFRP retrofitting effect on the dynamic characteristics of model steel structure", *Steel and Compos. Struct.*, **28**(2), 223-231. https://doi.org/10.12989/scs.2018.28.2.223.

Tuhta, S. (2019), "OMA of model chimney using Bench-Scale earthquake simulator", *Earthq. Struct.*, **16**(3), 321-327. https://doi.org/10.12989/eas.2019.16.3.321.

Uzun, B. and Civalek, Ö. (2019), "Free vibration analysis Silicon nanowires surrounded by elastic matrix by nonlocal finite element method", *Adv. Nano Res.*, **7**(2), 99-108. https://doi.org/10.12989/anr.2019.7.2.099.

Wang, L., Guo, F., Lin, Y., Yang, H. and Tang, S.W. (2020a), "Comparison between the effects of phosphorous slag and fly ash on the CSH structure, long-term hydration heat and volume deformation of cement-based materials", *Constr. Build. Mater.*, **250**, 118807. https://doi.org/10.1016/j.conbuildmat.2020.118807.

Wang, L., Luo, R., Zhang, W., Jin, M. and Tang, S. (2020b), "Effects of fineness and content of phosphorus slag on cement hydration, permeability, pore structure and fractal dimension of concrete", *Fractals*, **29**(2), 2140004. https://doi.org/10.1142/S0218348X21400041.

Wang, L., Jin, M., Wu, Y., Zhou, Y. and Tang, S. (2021a), "Hydration, shrinkage, pore structure and fractal dimension of silica fume modified low heat Portland cement-based materials", *Constr. Build. Mater.*, **272**, 121952.
https://doi.org/10.1016/j.conbuildmat.2020.121952.

Wang, L., He, T., Zhou, Y., Tang, S., Tan, J., Liu, Z. and Su, J. (2021b), "The influence of fiber type and length on the cracking resistance, durability and pore structure of face slab concrete", *Constr. Build. Mater.*, **282**, 122706. https://doi.org/10.1016/j.conbuildmat.2021.122706.

Zhang, P., Wang, K., Wang, J., Guo, J., Hu, S. and Ling, Y. (2020), "Mechanical properties and prediction of fracture parameters of geopolymer/alkali-activated mortar modified with PVA fiber and nano-SiO_2", *Ceram. Int.*, **46(**12), 20027-20037. https://doi.org/10.1016/j.ceramint.2020.05.074.

Zhang, P., Gao, Z., Wang, J. and Wang, K. (2021), "Numerical modeling of rebar-matrix bond behaviors of nano-SiO_2 and PVA fiber reinforced geopolymer composites", *Ceram. Int.*, **47**(8), 11727-11737. https://doi.org/10.1016/j.ceramint.2021.01.012.

CC